

# Hydrogen Fluoride Chemical Laser Multiple-Pass Amplifier Performance

R. E. Waldo,\* L. H. Sentman,† P. T. Theodoropoulos,\* and D. L. Carroll\*  
University of Illinois, Urbana, Illinois 61801

The performance of a continuous wave hydrogen fluoride chemical laser master oscillator with power amplifier was measured as a function of input power, the number of passes through the gain medium, and location of the optical axis of the input beam. The amplification ratio is an inverse function of the input power (intensity) and, for maximum amplification, the peak of the intensity distribution must be matched to that of the zero power gain distribution in the amplifier. A substantial performance advantage was measured with two-pass amplification when the two passes overlapped at least 60% and filled less than 84% of the zero power gain zone of the amplifier. The measured two-pass  $P_{out}$  vs  $P_{in}$  performance curve was significantly above the single-pass data and showed that only one-sixth of a device's oscillator output must be input to obtain two-pass amplifier output equal to the device's oscillator performance. An amplifier performance model that predicts a device's amplifier performance given the device's oscillator performance as a function of reflectivity was extended to predict multiple-pass amplifier performance. The two-pass model predictions were in good agreement with the measured two-pass amplifier performance data. The predicted amplifier performance as a function of gain length was found to be independent of device and showed that, with a 1-m gain length, one oscillator may be able to drive as many as 12 two-pass amplifiers.

## Nomenclature

AR	= amplification ratio, $P_{out}/P_{in}$
$L_e$	= thickness of the mixed flow ( $= L_g$ when fully mixed)
$L_g$	= geometric gain length
$P_{in}$	= input power to the amplifier
$P_{outAMP}$	= $P_{out}$ = output power from the amplifier
$P_{outOSC}$	= output power from the oscillator
$R_{eff}$	= effective reflectivity of the oscillator's resonator, = reflectivity of the outcoupler mirror times that of the feedback mirror
$X_{ib}$	= distance between the optical axis of the input beam and the $H_2$ injectors of the amplifier
$\Delta$	= $P_{out} - P_{in}$
$\zeta_{in}$	= nondimensional input power, = $\frac{\text{input power to the amplifier}}{\text{output power from the oscillator at } R_{eff} = 20\%}$
$\zeta_{out}$	= nondimensional output power, = $\frac{\text{output power from the amplifier}}{\text{output power from the oscillator at } R_{eff} = 20\%}$

## I. Introduction

THE calculations presented in Refs. 1 and 2 showed how a device's single-pass amplifier performance,  $P_{out}$  vs  $P_{in}$  and AR vs  $P_{in}$ , increased as the device's gain length was scaled from 0.3 to 4 m. The results of these calculations showed that, independent of device, a 4-m laser may be able to drive as many as eight amplifiers if the amplifiers are to produce as much power as could be obtained by running them as oscillators. All of these results are based on single-pass amplification of the input beam. To determine the effect of multiple-pass amplification of the input beam on amplifier performance, the amplifier performance model presented in Refs. 1 and 2 was extended to predict multiple-pass amplifier performance. In particular, the amplifier performance of the University of Illinois at Urbana-Champaign (UIUC), Helios, and CL

XI lasers was calculated for two-, three-, and four-pass amplification of the input beam through the amplifier.

The multiple-pass amplifier performance calculations showed that amplifier performance increased with multiple-pass amplification of the input beam through the amplifier's gain medium. In particular, it was found that the  $P_{in}$  required to achieve amplifier  $P_{out}$  equal to the device's oscillator  $P_{outOSC}$  decreased with multiple-pass amplification. This result indicated that an oscillator can drive more amplifiers with multiple-pass amplification. To determine if this performance increase is realized experimentally, the amplifier performance of the UIUC CL II (a two-channel, arc-driven, subsonic, continuous-wave hydrogen fluoride chemical laser with a 30-cm gain length) was measured for two and three passes through the gain medium.

The analytical model to predict multiple-pass amplifier performance is introduced in Sec. II. Section III contains several multiple-pass amplifier performance calculations. The experimental multiple-pass amplifier performance data for three different alignment configurations are presented in Sec. IV. Several concluding remarks are given in Sec. V.

## II. Multiple-Pass Amplifier Model

The amplifier model<sup>1,2</sup> is based on the observation that the average gain in the amplifier will be the same as the saturated gain in the oscillator when the circulating radiative flux in the oscillator is the same as the average radiative flux in the amplifier. For a multiple-pass amplifier, the  $P_{out}$  for pass  $N - 1$  is the  $P_{in}$  for pass  $N$ . With the assumption that the optical paths of all the passes coincide, an approximation of the average radiative flux in the amplifier after  $N$  passes is given by

$$P_{avAMP} = \frac{1}{2} (P_{in} + P_{outN}) + \sum_{i=1}^{N-1} P_{outi} \quad (1)$$

where  $P_{in}$  is the initial  $P_{in}$  for pass one. Since the saturated gain in an oscillator is the same as the average gain in the amplifier when the circulating radiative flux in the oscillator is the same as the average radiative flux in the amplifier,

$$\alpha_{AMP} = \alpha_{SAT} = -\frac{1}{2L_e} \ell_n(R_{eff}) \quad (2)$$

Received Nov. 13, 1991; revision received March 4, 1993; accepted for publication March 9, 1993. Copyright © 1993 by the American Institute of Aeronautics and Astronautics, Inc. All rights reserved.

\*Research Assistant, Aeronautical and Astronautical Engineering Department. Member AIAA.

†Professor, Aeronautical and Astronautical Engineering Department. Associate Fellow AIAA.

With Eq. (2),

$$P_{out_i} = P_{out_{i-1}} e^{\alpha_{AMP} L_e} = P_{out_{i-1}} \sqrt[N]{R_{eff}} \quad (3)$$

From Eq. (3),  $P_{out_N}$  can be written as

$$P_{out_N} = \frac{P_{in}}{(R_{eff})^{N/2}} \quad (4)$$

The circulating power in the oscillator is

$$P_{circOSC} = \frac{P_{outOSC}}{1 - R_{eff}} = \frac{aR_{eff} + b}{1 - R_{eff}} \quad (5)$$

when  $P_{outOSC}$  is represented by a linear function of  $R_{eff}$ . Then by setting  $P_{avAMP} = P_{circOSC}$ , the substitution of Eqs. (3) and (4) for  $P_{out_i}$  and  $P_{out_N}$  and utilization of the expression for the sum of a geometric series to eliminate the summation give

$$\frac{P_{in}}{R_{eff}^{N/2}} = 2 \left[ \frac{aR_{eff} + b}{1 - R_{eff}} - \frac{P_{in}}{R_{eff}^{N/2}} \frac{(R_{eff}^{1/2} - R_{eff}^{N/2})}{(1 - R_{eff}^{1/2})} \right] - P_{in} \quad (6)$$

Equation (6) may be written as a polynomial in  $R_{eff}$  as

$$(P_{in} + 2a) R_{eff}^{(N+2)/2} + 2P_{in} R_{eff}^{(N+1)/2} + (P_{in} + 2b) R_{eff}^{N/2} - P_{in} R_{eff} - 2P_{in} R_{eff}^{1/2} - P_{in} = 0 \quad (7)$$

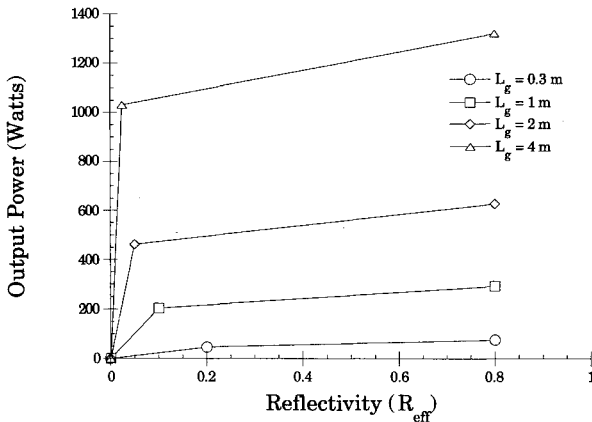


Fig. 1 Straight-line approximations to the oscillator performance of the UIUC laser for run 36 flow rates when scaled to large values of gain length  $L_g$ .

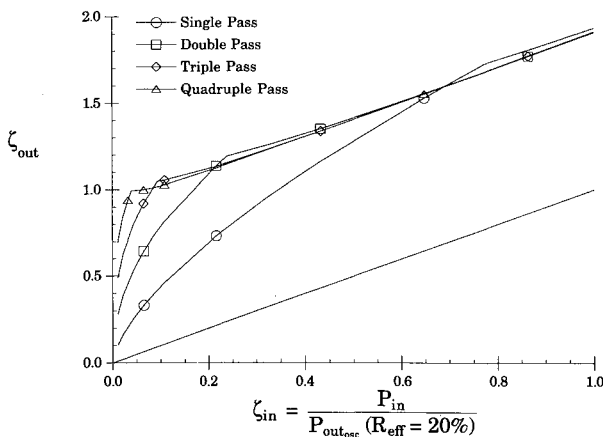


Fig. 2 Amplifier performance  $\zeta_{out}$  vs  $\zeta_{in}$  of the UIUC laser as a function of the number of passes through the amplifier for run 36 flow rates for a 30-cm gain length.

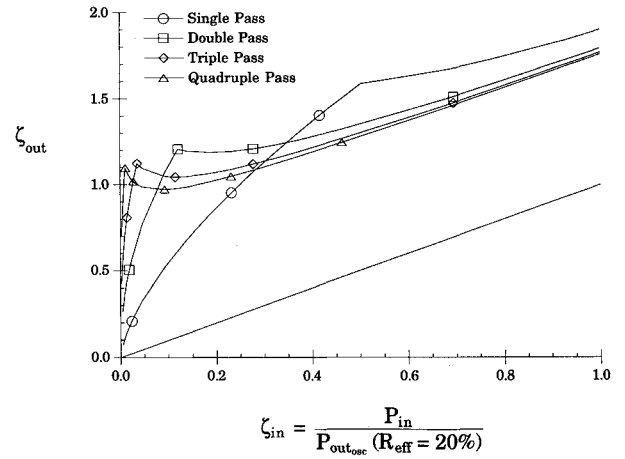


Fig. 3 Amplifier performance  $\zeta_{out}$  vs  $\zeta_{in}$  of the UIUC laser as a function of the number of passes through the amplifier for run 36 flow rates for a 1-m gain length.

For a given  $P_{in}$ ,  $a$  and  $b$ , Eq. (7) is solved for  $R_{eff}$ , which is then substituted into Eq. (4) to calculate  $P_{out_N}$  for the  $N$ -pass amplifier.

In the development of Eq. (7), it was assumed that the oscillator performance curve as a function of reflectivity could be represented by a sequence of straight lines, (Fig. 1). The location where two straight-line segments of the oscillator performance curve meet is called an intersection point. To solve Eq. (7) for  $R_{eff}$ , one must know which straight-line segment of the oscillator performance curve (the values of  $a$  and  $b$ ) to use for each  $P_{in}$ . This is accomplished by determining the value of  $P_{in}$  that corresponds to each intersection point of the oscillator performance curve. These values of  $P_{in}$  are determined by solving Eq. (6) for  $P_{in}$

$$P_{in} = \frac{2R_{eff}^{N/2} (aR_{eff} + b)}{(1 + R_{eff}^{1/2}) [(1 + R_{eff}^{N/2}) (1 - R_{eff}^{1/2}) + 2(R_{eff}^{1/2} - R_{eff}^{N/2})]} \quad (8)$$

When the values of  $R_{eff}$ ,  $a$  and  $b$ , at each intersection point are substituted into Eq. (8), the value of  $P_{in}$  for that intersection point is determined. Then, when Eq. (7) is solved for  $R_{eff}$ , comparison of the  $P_{in}$  with the  $P_{in}$  associated with the intersection points determines the  $a$  and  $b$  that should be used in Eq. (7). In the next section, this model is used to predict multiple-pass amplifier performance.

### III. Multiple-Pass Amplifier Performance Calculations

The single-pass amplifier performance model  $N = 1$ , which predicts a device's amplifier performance given the device's oscillator performance as a function of reflectivity, was solved in Refs. 1 and 2 and shown to give good agreement with the single-pass data. The effect of the oscillator performance on the calculated amplifier performance is explained in detail in Refs. 1 and 2. In particular, it was found that the oscillator performance in the range  $0 \leq R_{eff} \leq$  break point (the break point is the value of  $R_{eff}$  at which the oscillator power vs  $R_{eff}$  curve first becomes linear with  $R_{eff}$ , i.e., the first intersection point) determined the amplifier performance in the range of interest.

To determine the effect of multiple-pass amplification on amplifier performance, the multiple-pass amplifier model, Eqs. (7) and (4), was used to calculate the performance of the UIUC, Helios, and CL XI lasers with double-, triple- and quadruple-pass amplification of the input beam for gain lengths of 0.3, 1, 2, and 4 m. In Refs. 1 and 2, it was shown that for the three devices, the break points could be chosen to occur at a value of  $R_{eff}$  of 20% for the 0.3-m laser, 10% for the 1-m laser, 5% for the 2-m laser and 2.5% for the 4-m laser. Figure 1 shows the straight-line approximation of the BLAZE II (a quasi-two-dimensional, finite-rate, mixing, chemical laser simulation code) theoretical oscillator performance calculations (anchored to 0.3-m data and used to scale to 1, 2, and 4 m) for the UIUC laser.<sup>1,2</sup>

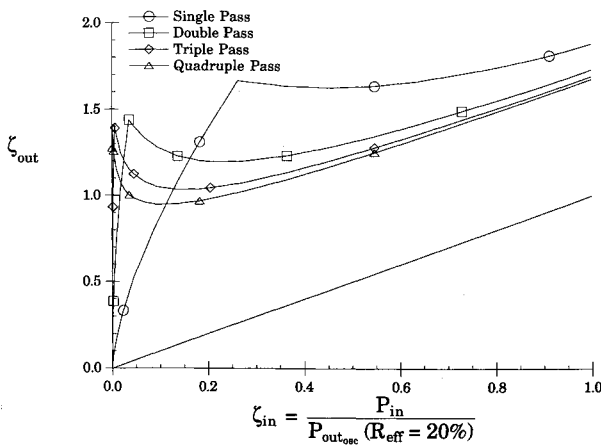


Fig. 4 Amplifier performance  $\zeta_{out}$  vs  $\zeta_{in}$  of the UIUC laser as a function of the number of passes through the amplifier for run 36 flow rates for a 4-m gain length.

The oscillator performance curves shown in Fig. 1 were used as input to the multiple-pass amplifier model. The calculated 0.3-, 1-, and 4-m UIUC amplifier performance  $\zeta_{out}$  vs  $\zeta_{in}$  is shown in Figs. 2, 3, and 4, respectively. These figures show the amplifier performance for single-, double-, triple-, and quadruple-pass amplification of the input beam. To obtain the  $\zeta_{out}$  vs  $\zeta_{in}$  curves, the calculated  $P_{out}$  vs  $P_{in}$  curves were nondimensionalized with the devices' oscillator performance with a 20% reflective outcoupler,  $R_{eff} = 20\%$  (the  $R_{eff}$  value used to select the reference value of  $P_{out,osc}$  is arbitrary as long as the same value of  $R_{eff}$  is used for all gain lengths and devices).

Comparison of Figs. 2–4 shows that for small  $\zeta_{in}$ ,  $\zeta_{out}$  increases with the number of passes the input beam makes through the gain medium. This behavior is similar to but more dramatic than the effect of increasing gain length.<sup>1,2</sup> Specifically, the  $\zeta_{out}$  vs  $\zeta_{in}$  plots show that, for a fixed  $L_g$ , the value of  $\zeta_{in}$  at which the amplifier performance curve first reaches a value of  $\zeta_{out} = 1$  decreases with the number of passes through the gain medium. For a fixed number of passes through the gain medium, these plots show that the value of  $\zeta_{in}$  at which the amplifier performance curve first reaches a value of  $\zeta_{out} = 1$  decreases as  $L_g$  increases because  $R_{eff}$  at the break point decreases with gain length.

Amplifier performance for the 4-m Helios and 4-m CL XI lasers was calculated as a function of the number of passes. When these performance curves were superimposed<sup>2</sup> with Fig. 4, it was shown that for three different devices all with the same gain length, one set of curves results independent of the device when the break point occurs at the same  $R_{eff}$  (2.5%) for all of the devices. This demonstrates that amplifier performance for a fixed gain length is device independent; thus, the amplifier performance curves shown in Figs. 2–4 are device independent.

The device-independent curves in Figs. 2–4 were used to calculate the number of amplifiers an oscillator can drive as a function of the number of passes through the gain medium and gain length (Fig. 5). Since this figure is device independent,<sup>2</sup> it can be used to determine the required gain length and number of passes to achieve a desired MOPA system performance. Figure 5 shows that there is a definite performance advantage to multiple-pass amplification.

#### IV. Experimental Multiple-Pass Amplifier Performance

The calculations presented in Sec. III showed that amplifier performance increased with multiple-pass amplification of the input beam through the amplifier's gain medium. To determine if this performance increase is realized experimentally, the amplifier performance of the UIUC CL II was measured for two and three passes through the gain medium. To fully characterize the multiple-pass amplifier, amplifier performance was measured as a function of input power, location of the optical axis of the input beam,

and orientation of the optical axis of each additional pass with respect to the input beam. The two-pass amplifier performance was measured for three different alignment schemes: 1) "collinear," 2) "tilted," and 3) "crossed." The three-pass amplifier performance was measured with the cross-alignment scheme and will be presented last.

The oscillator used for all of the multiple-pass amplifier experiments was the CL I.<sup>3</sup> The CL I's multiline stable resonator alignment is described in Ref. 4. The oscillator's output beam was aligned and then injected into the amplifier with a 2-m convex lens. The alignment was such that there was zero clipping of the input beam by the amplifier's flow channel. The alignment of the input beam from the oscillator to the amplifier is described in Ref. 5. For each experiment, the input beam was initially aligned through the amplifier so that the axis (center) of the input beam was aligned parallel with the hydrogen ( $H_2$ ) injectors at the location of the  $H_2$  injectors (nozzle exit plane) of the amplifier. This location of the optical axis is defined as  $X_{ib} = 0.0$  ( $X_{ib}$  is the distance in millimeters between the optical axis and  $H_2$  injectors or nozzle exit plane). This alignment was accomplished by placing graph paper at the entrance (location 7) and exit (location 8) of the CL II and allowing the IR beam to burn through the paper. The alignment of the IR beam was adjusted until the paper showed that the IR beam was parallel to the  $H_2$  injectors and centered in the flow channel.

Amplifier performance as a function of the location of the axis of the input beam was obtained by translating the entire optical bench to which the turning mirror, 2-m convex lens, beam splitter (BS) and plano total reflector were attached.<sup>5</sup> Different input powers to the amplifier ( $P_{in}$ ) were obtained by placing partially transmissive mirrors in the path of the beam between the oscillator and amplifier and varying the flow rates in the oscillator.

The two-pass amplifier experiments that were performed with the collinear alignment were unsuccessful. It was found that the CL II amplifier was operating as an oscillator by lasing between the plano total reflector and the backside of the CL I's 73% reflective outcoupler and between the plano total reflector and CL I's 2-m radius of curvature, concave (cc) enhanced total reflector (ETR). Even though the effective reflectivity of this cavity was less than 10%, the CL II lased because of its large 18%/cm gains.<sup>5</sup> This demonstrates a difficulty that may arise in any collinear two-pass amplifier system. To solve this problem, tilted and crossed alignment configurations were devised.

##### A. Tilted Two-Pass Amplifier Performance

To prevent the CL II from lasing, the plano total reflector mirror was adjusted so that the second-pass beam was slightly tilted. This tilt of the second-pass beam allowed a knife edge to be placed in the beam's path to prevent the second pass from reaching the 73%

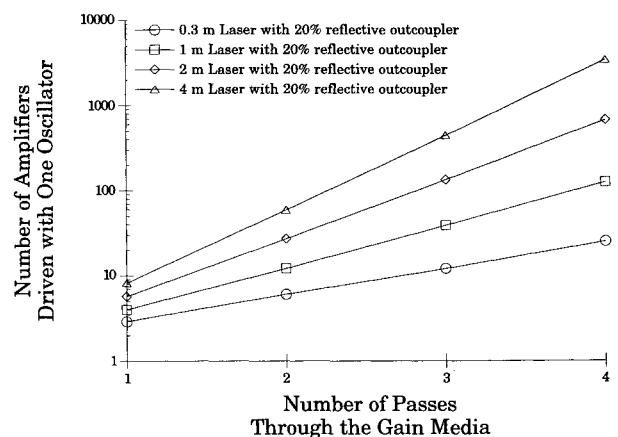


Fig. 5 Number of amplifiers one oscillator can drive and obtain amplifier performance that is equal to the performance that could be obtained by running the device as an oscillator as a function of the number of passes through the amplifier for a 0.3-, 1-, 2-, and 4-m gain length laser.

reflective outcoupler (Fig. 6). The use of the knife edge and tilted alignment prevented the CL II from lasing; however, the CL II did lase with a tilted alignment if the knife edge was not used. Power and spectra were monitored at locations 5 and 10 to determine the two-pass amplifier performance.

CL II amplifier performance was measured for two tilt angles of the feedback beam,  $\alpha = 7.47$  mR (tilted alignment 1) and 3.74 mR (tilted alignment 2). A tilt angle of 3.74 mR was the minimum angle that allowed the knife edge to completely block the feedback beam (without the knife edge clipping the incoming beam).  $P_{out}$  as a function of  $P_{in}$  is plotted in Fig. 7 for these two configurations. Figure 7 shows that at about the same  $P_{in}$ , the amplifier performance increased when the tilt angle was reduced (the scatter of the data represents the repeatability of the experiment). Spectra at the  $X_{ib}$  for peak AR indicated that the amplifier has little effect on the spectra, a result consistent with the single-pass data.<sup>3,5,6</sup> These results imply that maximum performance should be achieved when both passes are collinear or maximum performance will occur when the percentage overlap of both passes is maximized. This is explained by the fact that when the two beams have maximum overlap, a maximum intensity is developed, which in turn stimulates the maximum emission of radiation from the amplifier's gain medium.

The idea behind the collinear alignment of the two-pass amplifier was to obtain maximum overlap of the first- and second-pass beams. Since data could not be obtained with a collinear alignment (because the CL II lased), it was necessary to devise an alignment scheme that would prevent the CL II from lasing and yield a good overlap of the first- and second-pass beams. The percent overlap of

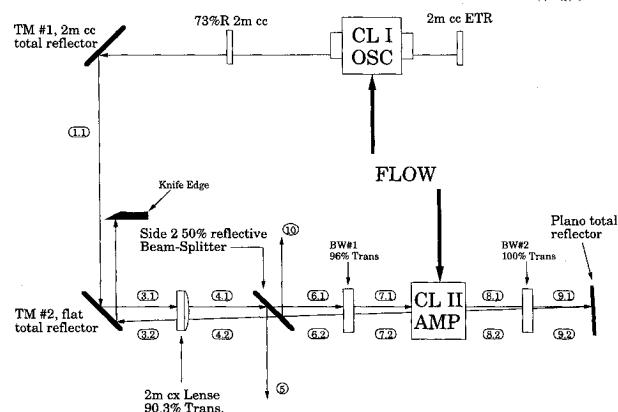


Fig. 6 Diagram of the experimental layout for the tilted two-pass amplifier experiments that shows the feedback beam from the plano total reflector back to the knife edge.

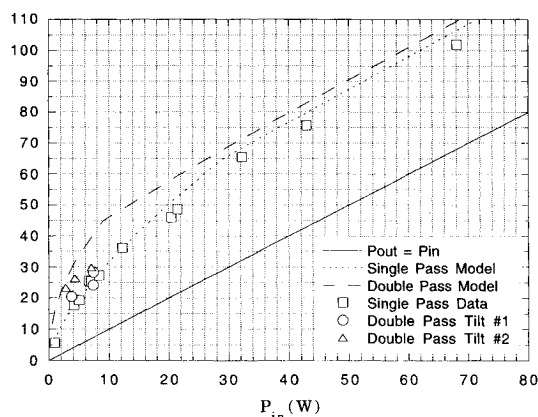


Fig. 7 Output power vs input power at the  $X_{ib}$  for peak amplification for run 36 flow rates in the amplifier for tilted beam alignments 1 and 2.

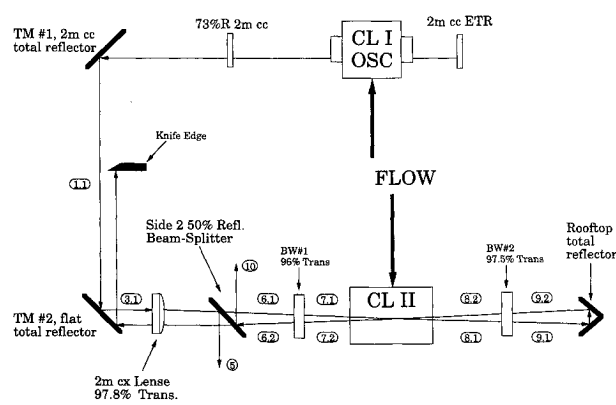


Fig. 8 Diagram of the experimental layout for the two-pass experiments with the crossed beam alignment that shows the feedback beam from the rooftop mirror back to the knife edge.

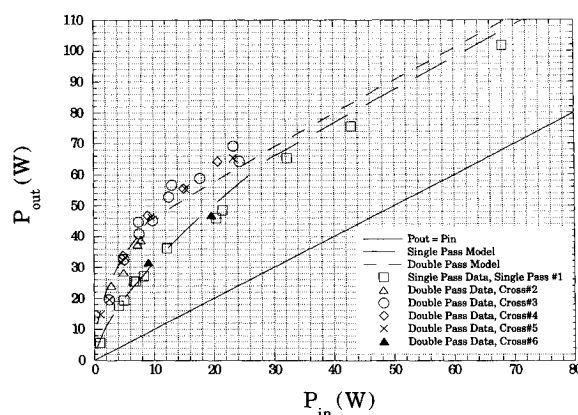


Fig. 9 Output power vs input power at the  $X_{ib}$  for peak amplification for run 36 flow rates in the amplifier for several crossed-beam alignments.

the first- and second-pass beams for a given alignment scheme was determined as follows. The two-dimensional area of overlap of the beams in the plane that contains the optical axes of both beams was calculated. Then the two-dimensional area of one of the beams in the same plane was calculated [since the focal point of the 2-m convex lens was at the plano total reflector (location 9.1) (Fig. 6), the geometry of the first- and second-pass beams and therefore their two-dimensional areas were the same]. The percentage overlap of the two beams is given by the ratio of the area of overlap to the two-dimensional area of either of the beams. The percentage overlap for tilted beam alignments 1 and 2 was calculated as 19.3 and 58.9%, respectively. The next section presents an alignment that increased the percentage overlap of the first- and second-pass beams.

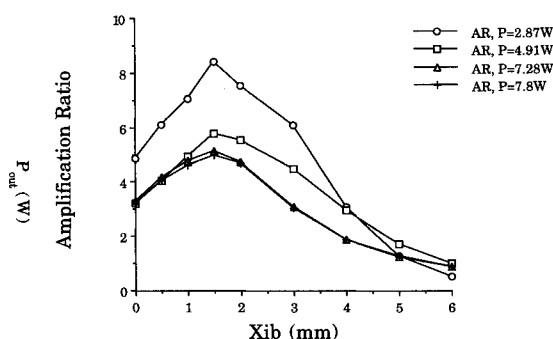
## B. Crossed Two-Pass Amplifier Performance

To increase the overlap of the first- and second-pass beams, a crossed-beam alignment scheme was developed (Fig. 8). The purpose of this alignment was to have the two beams cross in the middle of the amplifier's flowfield, which would give good overlap of the two beams for a significant portion of the amplifier gain zone. For this alignment, beam 1 was aligned so that it entered the amplifier 0.5 mm upstream of the  $H_2$  injectors and exited the amplifier 0.5 mm downstream of the  $H_2$  injectors. The plano total reflector was replaced by a rooftop mirror that consisted of two plano total reflectors mounted approximately 90 deg to each other. This allowed beam 2 to enter the amplifier 0.5 mm upstream of the  $H_2$  injectors and exit the amplifier 0.5 mm downstream of the  $H_2$  injectors. Both beams were centered vertically in the flow channel. The percentage overlap for crossed-beam alignment 2 was 84.6%. To

**Table 1** Comparison of various parameters as a function of the alignment for one-, two-, and three-pass amplification

Alignment no.	Alignment name	Number of passes	Angle between beams, mR	% Overlap	Average width of beam, mm	% of ZPG zone filled by the beam	Comparison to analytic results
1	Single 1	1	—	—	2.50	46.3	Equal to single-pass model
2	Single 2	1	—	—	3.25	60.2	Equal to single-pass model
3	Tilted 1	2	7.47	19.3	5.93	109.8	Equal to single-pass model
4	Tilted 2	2	3.74	58.9	4.59	85.0	Close to double-pass model
5	Cross 2	2	5.62	84.6	3.79	70.2	Equal to double-pass model
6	Cross 3	2	13.36	61.0	4.53	83.9	Equal to double-pass model
7	Cross 4	2	11.24	69.2	4.25	78.7	Equal to double-pass model
8	Cross 5	2	11.24	69.2	4.25	78.7	Equal to double-pass model
9	Cross 6	2	16.88	44.0	5.13	95.0	Equal to single-pass model
10	Cross 7	2	15.40	57.8	4.65	86.1	Close to double-pass model
11	Cross 8	2	14.00	61.5	4.50	83.1	Close to double-pass model
12	Cross 7.1	3	—	25.03	5.76	106.7	Equal to single-pass model
13	Cross 8.1	3	—	19.8	5.88	108.97	Equal to single-pass model

The average width of the CL II low-pressure zero power gain zone for lines  $P_1$  (5-9) and  $P_{21}$  (5-9) is 5.4 mm.

**Fig. 10** Amplification ratio vs  $X_{ib}$  and  $P_{in}$  for run 36 flow rates in the amplifier for crossed-beam alignment 2.

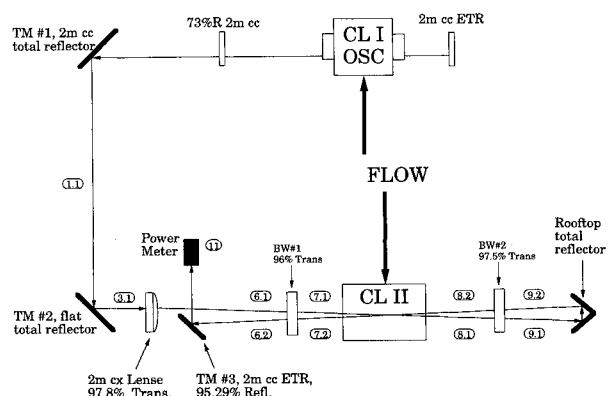
ensure that the CL II did not lase, a knife edge was placed in the beam's path (Fig. 8).

CL II amplifier performance was measured with this crossed beam alignment.  $P_{out}$  as a function of  $P_{in}$  and AR vs  $X_{ib}$  are plotted in Figs. 9 and 10, respectively. Figure 9 shows that the two-pass data and model are in reasonable agreement, i.e., the model predicts the magnitude and character of the two-pass amplifier performance. Figure 10 illustrates that the location of the peak AR occurs at an  $X_{ib}$  of 1.5 mm, which is the result obtained for the single-pass amplifier.<sup>3,5,6</sup> Spectra at the  $X_{ib}$  for peak AR indicated that the amplifier has little effect on the spectra, a result consistent with the single-pass data.<sup>3,5,6</sup> The next step was to obtain data at higher input powers ( $> 10$  W). Because of the 50% beam splitter, the maximum input power that the probe laser could provide was 7.8 W.

When the beam splitter was removed, the input power to the amplifier was increased by a factor of 3. Without the BS, the beam was outcoupled by a scraper mirror at location 6.2 (Fig. 11). The separation distance required between the two beams so that the scraper mirror did not clip the first-pass beam at location 6.2 dictated the minimum cross-angle between the two beams.

With this new configuration, CL II amplifier performance was measured for a range of  $P_{in}$ , from 2.52 to 24.38 W, for crossed alignments 3 and 4. The difference between cross alignments 3 and 4 is the angle between the two beams. The characteristics of each alignment are summarized in Table 1.  $P_{out}$  as a function of  $P_{in}$  data for both of these alignments is plotted in Fig. 9.  $P_{in}$ , the power at location 7.1 (Fig. 11), is determined by measuring the power at location 9.1 with  $H_2$  off and calculating the power at location 7.1 by the following equation:

$$P_{7.2} = P_{11} \times \frac{1}{\#2 \text{ BW Trans}} \quad (9)$$

**Fig. 11** Diagram of the experimental layout for the two-pass experiments with the crossed beam alignment that shows the feedback beam from the rooftop mirror back to the scraper mirror that outcouples the feedback beam.

$P_{out}$ , the power at location 7.2 (Fig. 11), is determined by measuring the power at location 11 with  $H_2$  on and calculating the power at location 7.2 by the following equation:

$$P_{7.2} = P_{9.1} \times \frac{1}{\text{TM \#3 Refl}} \times \frac{1}{\#1 \text{ BW Trans}} \quad (10)$$

The amplification ratio is  $P_{out}/P_{in}$ . Figure 9 shows that the two-pass amplifier data agree well with those of the two-pass amplifier model. These data demonstrate the increase in performance over single-pass amplification. For all three of the cross-alignments, 2, 3, and 4, the first-pass beam was aligned so that it entered the amplifier some distance upstream of the  $H_2$  injectors and exited the amplifier some distance downstream of the  $H_2$  injectors; the second-pass beam was aligned so that it entered the amplifier some distance upstream of the  $H_2$  injectors and exited the amplifier some distance downstream of the  $H_2$  injectors. To determine if this particular orientation of the beams was important to performance, the exact opposite alignment was used to measure amplifier performance, i.e., the beams were aligned downstream to upstream. This alignment is designated cross alignment 5 (Table 1).

CL II amplifier performance was measured for a range of  $P_{in}$  from 1.04 to 23.29 W with crossed alignment 5.  $P_{out}$  as a function of  $P_{in}$  data is plotted in Fig. 9. Figure 9 shows that these data agree well with the two-pass amplifier data obtained with cross alignments 2, 3, and 4.

These results define the maximum CL II two-pass amplifier performance for various cross alignments. To determine the sensitivity of the two-pass amplifier performance to the overlap of the

two beams, two-pass amplifier performance was measured with cross-beam alignment 6 (Table 1). CL II amplifier performance was measured for  $P_{in}$  of 9.11 and 19.67 W with crossed alignment 6.  $P_{out}$  as a function of  $P_{in}$  data is plotted in Fig. 9. Figure 9 shows that these data are much lower than the two-pass amplifier data obtained with previous cross alignments and that the data agree well with the single-pass data.

The amplifier performance data for all the different alignments suggest that the important alignment parameters for the two-pass amplifier are the percentage overlap of the two beams and the percentage of the zero power gain (ZPG) zone filled by the two beams. To determine how these parameters vary with alignment, a comparison of the percentage overlap of the two beams for the different alignments and a comparison of the average width of the entire two-pass beam to that of the ZPG zone are given in Table 1. This table shows that to obtain maximum performance, the two beams should have more than 60% overlap and fill less than 84% of the ZPG zone, i.e., the best alignment is one that fills a significant portion of the ZPG zone with a maximum intensity, a physically reasonable result.

The CL II oscillator performance<sup>3</sup> at run 36 flow rates with a 20% reflective outcoupler is 36 and 68 W (maximum output power) with a 73% reflective outcoupler. Figure 9 shows that to obtain a total power of 36 W after the amplifier, about 6 W must be input and to obtain 68 W after the amplifier, about 23 W must be input. These data show that one oscillator can drive between three and six two-pass amplifiers and obtain amplifier output equal to the device's oscillator performance when the oscillator is operated with a 20 and 73% reflective outcoupler, respectively. This research is a factor of 2 increase over the single-pass results.<sup>3,5,6</sup>

Figure 12 shows that, for the CL II gain cell at run 36 flow rates, the maximum power extracted from the single-pass amplifier is 33.2 W, and that from the two-pass amplifier is 46.4 W. The minimum oscillator power is 68 W.<sup>3</sup> Therefore, operating the CL II as a

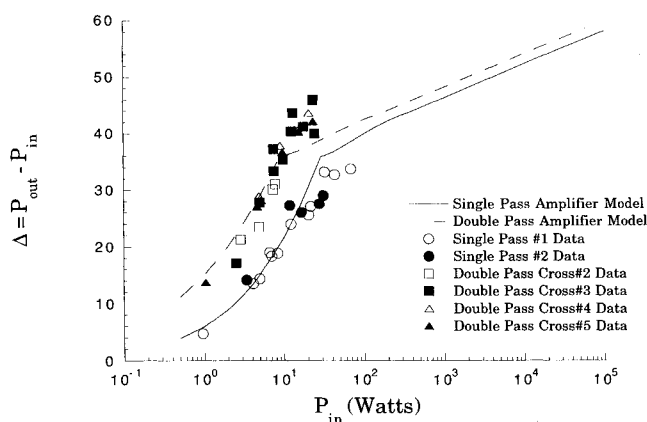


Fig. 12 Experimental and calculated  $\Delta$  vs input power for one- and two-pass amplification at the  $X_{ib}$  for peak AR for run 36 flow rates in the amplifier.

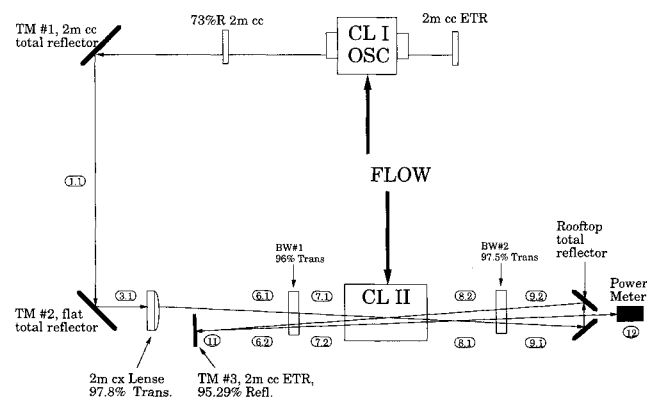


Fig. 13 Diagram of the experimental layout for the three-pass amplifier experiments.

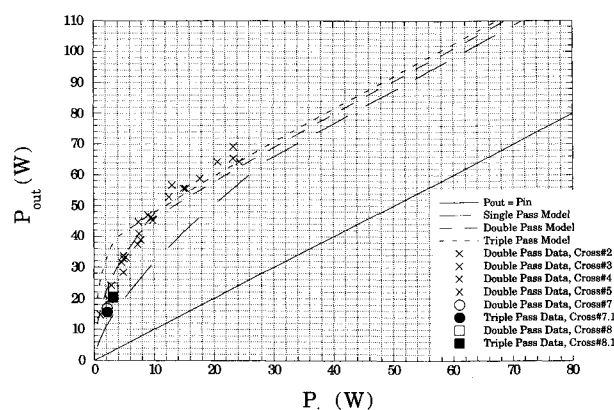


Fig. 14 Output power vs input power at the  $X_{ib}$  for peak amplification for run 36 flow rates in the amplifier for crossed-beam alignments 7 and 8 (two pass) and crossed-beam alignments 7.1 and 8.1 (three-pass).

\*two-pass amplifier extracts about 68.2% of the available energy in the flow for the range of  $P_{in}$  measured, representing a 40% increase in energy extraction over single-pass amplification. The model calculations in Fig. 12 show the slow increase in  $\Delta$  as  $P_{in}$  increases. Unfortunately, the large values of  $P_{in}$  required to obtain larger  $\Delta$  are of no practical interest.

### C. Three-Pass Amplifier Performance

Data presented in the last section showed that two-pass amplifier performance is significantly higher than single-pass performance. The amplifier performance model agreed well with these data. Since the model predicts another increase in performance with a third pass, three-pass amplifier performance was measured.

The experimental layout required to obtain three-pass alignment is shown in Fig. 13. To allow the third-pass beam to pass between the rooftop mirrors without clipping, the rooftop mirrors had to be separated by 4.0 mm. These mirrors touched each other during the two-pass experiments. With these mirrors separated, the first- and second-pass alignments were controlled by the restriction that no part of the first- or second-pass beams should pass between the rooftop mirrors and that the first and second passes must have maximum overlap, greater than 60%. The two-pass alignment that could be obtained that best satisfied these requirements is denoted cross 7 (Table 1). Before the third-pass alignment was attempted, two-pass amplifier performance data were obtained so that the performance of each pass could be quantified for this particular alignment.

CL II amplifier performance was measured at an input power of 2.17 W.  $P_{out}$  as a function of  $P_{in}$  data is plotted in Fig. 14. Figure 14 shows that this data point is slightly lower than the established performance. It was illustrated in the preceding section that to obtain maximum two-pass performance, the two beams must have better than 60% overlap and not fill more than 84% of the ZPG zone. With these criteria, the slightly lower performance can be explained with Table 1. Table 1 shows that cross alignment 7 is below the 60% overlap of the two beams and above the 84% of the ZPG zone filled by the beam criteria, which suggest lower performance. Because of the geometric restrictions on the alignment, this was the best alignment attainable.

With the two-pass amplifier performance measured, the third-pass was aligned. The three-pass alignment is denoted cross 7.1.  $P_{out}$  as a function of  $P_{in}$  data is plotted in Fig. 14. Figure 14 shows that the data are lower than the corresponding two-pass data. The lower performance is explained with Table 1, which shows that the overlap is only 25% and the beam fills 106.7% of the ZPG zone.

For the preceding three-pass data, the first-pass beam was aligned so that it entered the amplifier 1.0 mm downstream of the  $H_2$  injectors and exited the amplifier 1.5 mm upstream of the  $H_2$  injectors; the second-pass beam was aligned so that it entered the amplifier 1.5 mm downstream of the  $H_2$  injectors and exited the amplifier 1.5 mm upstream of the  $H_2$  injectors. The third-pass en-

tered the amplifier 1.75 mm upstream of the  $H_2$  injectors and exited the amplifier 1.0 mm upstream of the  $H_2$  injectors. To determine if this particular orientation of the beams was important to performance, the exact opposite alignment was used to measure amplifier performance, i.e., the beams would be aligned upstream to downstream. The two-pass part of this alignment is designated cross 8 (Table 1). Before the third-pass alignment was attempted, two-pass amplifier performance data were obtained so that the performance of each pass could be quantified for this particular alignment.

CL II amplifier performance was measured at an input power of 3.21 W.  $P_{out}$  as a function of  $P_{in}$  data is plotted in Fig. 14. Figure 14 shows that the data agree with the established two-pass performance. Because of the geometric restrictions on the alignment, this was the best alignment attainable.

With the two-pass amplifier performance measured, the third-pass was aligned, cross 8.1 (Table 1).  $P_{out}$  as a function of  $P_{in}$  data is plotted in Fig. 14. Figure 14 shows that the data are lower than the corresponding two-pass data. The lower performance is explained with Table 1, which shows that the overlap is only 19.8% and the beam fills 108.9% of the ZPG zone, which suggests lower performance.

These data show that the predicted increase in performance due to the third pass was not realized because it was not possible with the lasers and optics available to arrange the three passes with at least 60% overlap of the three beams and fill not more than 84% of the ZPG zone and still outcouple the third pass. With different equipment so that the overlap and gain zone fill requirements would be satisfied, it is anticipated that the predicted three-pass performance increase would be obtained.

## V. Concluding Remarks

Experimental two-pass amplifier performance was measured for three different alignment schemes: collinear, tilted, and crossed. When the amplifier was operated with the collinear alignment, the amplifier lased between the amplifier's second-pass feedback mirror and the oscillator's resonator mirrors; therefore, no valid amplifier data were obtained with this alignment. Amplifier data were obtained with the other two alignments because the second-pass beam could be blocked from returning to the oscillator optics.

The amplifier performance data for all of the different alignments indicate that the important alignment parameters for the two-pass amplifier are the percentage overlap of the two beams, percentage of the ZPG zone filled by the two beams, and the optical axis location. It was shown that to obtain maximum performance, the two beams should have more than 60% overlap and fill less than 84% of the ZPG zone and the optical axis of the two-pass beam should be centered on the peak of the ZPG distribution in the amplifier.

The two-pass amplifier data show that one oscillator can drive between three and six amplifiers and obtain amplifier output equal to the device's oscillator performance when the oscillator is operated with a 20 and 73% reflective outcoupler, respectively. This represents a factor of 2 increase over the single-pass results.

These data show that operating the CL II as a two-pass amplifier extracts about 68.2% of the available energy in the flow for the range of  $P_{in}$  measured. This is a 40% increase in energy extraction over single-pass amplification.

The single-pass amplifier performance model was extended to predict multiple-pass amplifier performance. Device-independent amplifier performance curves show that there is a definite performance advantage to multiple-pass amplification in the range of interest. The two-pass model predictions were in good agreement with the measured two-pass amplifier performance data. One oscillator can drive more amplifiers by increasing the number of passes the input beam makes through the amplifier's gain medium. The predicted amplifier performance as a function of gain length was found to be independent of device and that with a 1-m gain length, one oscillator may be able to drive as many as 12 two-pass amplifiers.

## Acknowledgments

This work was supported by the Strategic Defense Initiative Organization through W. J. Schafer Associates subcontract SC-88K-33-004 and by the University of Illinois.

## References

- <sup>1</sup>Waldo, R. E., and Sentman, L. H., "Effect of Gain Length on HF Chemical Laser Amplifier Performance," *AIAA Journal*, Vol. 31, No. 11, 1993, pp. 2090-2097.
- <sup>2</sup>Waldo, R. E., Sentman, L. H., Theodoropoulos, P. T., and Carroll, D. L., "On the Performance Characteristics of Multiple Pass HF Chemical Laser Master Oscillator/Power Amplifiers," TR 91-6, UILU Eng. 91-0506, Aeronautical and Astronautical Engineering Dept., Univ. of Illinois, Urbana, IL, Aug. 1991.
- <sup>3</sup>Sentman, L. H., Waldo, R., Nguyen, T., and Theodoropoulos, P., "cw HF Chemical Laser Oscillator/Amplifier Performance in a MOPA Configuration," TR 88-7, UILU Eng 88-0507, Aeronautical and Astronautical Engineering Dept., Univ. of Illinois, Urbana, IL, July 1988.
- <sup>4</sup>"Helios Models CL I and CL II Laboratory Chemical Laser Systems Installation and Operating Manual," Helios Inc., Longmont, CO, May 1981.
- <sup>5</sup>Sentman, L. H., Theodoropoulos, P., Waldo, R., Nguyen, T., and Snipes, R., "An Experimental Study of cw HF Chemical Laser Amplifier Performance and Zero Power Gain," TR 87-6, UILU Eng. 87-0506, Aeronautical and Astronautical Engineering Dept., Univ. of Illinois, Urbana, IL, Aug. 1987.
- <sup>6</sup>Sentman, L. H., Waldo, R. E., Theodoropoulos, P. T., Nguyen T. X., and Carroll, D. L., "HF Chemical Laser Amplifier Performance: Experiment," *AIAA Journal*, Vol. 30, No. 1, 1992, pp. 138-144.